CrossMark

Effect of the addition of a second phenol on the textural properties of carbon aerogels

N. Vera-Hincapié[1] · E. Romero-Malagón[1] · F. Carrasco-Marín[2] · Y. Agámez-Pertuz[1] ·
J. Díaz-Velásquez[1]

Abstract Three carbon aerogels (AGC) were prepared using the sol–gel method from the polymerization of mixtures of resorcinol–catechol (RC), resorcinol-*m*-cresol, and resorcinol–phloroglucinol (RP). Cobalt acetate was used as polymerization catalyst. The porous texture and the morphology of carbon aerogels were characterized by nitrogen adsorption at 77 K, carbon dioxide at 273 K and scanning electron microscopy. Their structure and chemical surface were analyzed by means of X-ray diffraction and X-ray photoelectron spectroscopy. It was found that the addition of a second phenol influences the porosity of the material. The carbon aerogel prepared with *m*-cresol as a monomer presented constrictions at the entrance of the micropores and lower pore volume compared to that of RC and RP. This fact is possibly due to the presence of the methyl group. Moreover, this monomer favors the formation of carbon fibers.

Keywords Carbon aerogels · Polymerization · Porosity · Gas adsorption · Textural properties

✉ Y. Agámez-Pertuz
yyagamezp@unal.edu.co

1. Laboratorio de Investigación en Combustibles y Energía, Departamento de Química, Universidad Nacional de Colombia, 11001 Bogotá D. C., Colombia

2. Grupo de Investigación en Materiales de Carbón, Departamento de Química Inorgánica, Universidad de Granada, 18001 Granada, Spain

1 Introduction

AGC are nanostructured materials obtained by sol–gel polycondensation of phenolic compounds with formaldehyde and a subsequent carbonization (Pekala and Alviso 1992). Among the advantages of the sol–gel process, its purity, homogeneity and control of the porosity of the materials are outstanding. In the case of the AGC obtained by this method, the development of a wide surface area, continuous porosity and electrical conductivity (Hanzawa et al. 1998) are remarkable. Thanks to these properties, these materials have a wide range of applications: heat and acoustic insulators, adsorbents, double-layer capacitors, molecular sieves and catalysts support (Feng et al. 2011; Moreno-Castilla and Maldonado-Hódar 2005; Pekala et al. 1998).

The most extensively studied AGC have been those synthesized from resorcinol–formaldehyde and melamine–formaldehyde, and their reaction parameters are the best understood ones (Leventis 2011; Tamon et al. 1997). However, research has been made in the use of other phenolic monomers, due to the high price of resorcinol. Li et al. (2002) employed mixtures of resorcinol/*m*-cresol and found out that 70 % of resorcinol can be replaced by *m*-cresol and that the characteristics of the resulting aerogels are similar to those of aerogels synthesized with 100 % resorcinol. Jirglová et al. (2009) have prepared AGC from phloroglucinol–phenol–formaldehyde mixtures and have found out that microporous–mesoporous materials can only be obtained from mixtures with high percentages of phloroglucinol.

Apart from the replacement of resorcinol by other phenols, another area of great interest in the synthesis of AGC is the incorporation of metal species inside the carbonaceous structure with the purpose of modifying their

properties, electrical conductivity and catalytic activity, achieved following different methods, such as the one suggested by Maldonado-Hódar et al. (2000). Applying this method, the metal is distributed through the porosity of the carbonaceous phase. Additionally, the added metal can catalyze the polymerization and gelation processes, which consequently affect the morphology and porous texture of the material.

In order to find more economical AGC and with adequate textural properties that allow them to be used as molecular sieves, the present study shows the effect of the addition of a second phenol on the superficial area, micropore volume, pore size distribution and morphology of AGC prepared with mixtures of resorcinol–catechol (RC), resorcinol-m-cresol (RmC), resorcinol–phloroglucinol (RP) and formaldehyde, employing cobalt acetate as a polymerization catalyst.

2 Experimental part

2.1 AGC synthesis

AGC were synthesized by polycondensation of phenolic compound mixtures (RC, RmC, and RP) with formaldehyde (F), employing cobalt acetate as a polymerization catalyst and deionized water (W) as the reaction medium. Molar relations between resorcinol and each of the other phenols were 1:1. RC/F, RmC/F and RP/F remained equal to 0.5, whereas the relations of RC/W and RmC/W were 0.13 and that of RP/W was 0.07, due to the fact that polymerization with phloroglucinol is very fast. The amount of cobalt acetate used was the one required to obtain 2.5 % of cobalt in the original mixture.

Resorcinol (Panreac, 99 %), m-cresol (Merck 98 %), phloroglucinol (Aldrich 97 %), formaldehyde (Panreac, 37 % in water), cobalt acetate (Merck, 99 %) and deionized water were used in the preparation of the mixture.

In order to synthesize the AGC, the phenolic monomers were mixed and cobalt acetate and formaldehyde were added subsequently, until a homogenous solution was obtained, which was poured in glass tubes (40 cm long and 0.5 cm i.d.). The tubes were sealed and subjected to a gelation process for one first day at 298 K, after that, for 2 days at 323 K and, finally, at 353 K for 5 days.

After the gelation phase, the gel bars were removed from the molds and cut into pellets measuring 1 cm long approximately, which were immersed in acetone, renewed each 10 h, during 3 days. In this process, the water present in the pores of the gel was replaced by acetone. This replacement was necessary to carry out the drying with supercritical carbon dioxide. Subsequently, the aerogels were dried with supercritical CO_2.

In order to obtain the AGC, the organic aerogels were carbonized at 1073 K during 5 h, with a N_2 stream of 100 mL/min, employing a heating rate of 1 K/min to allow the slow elimination of gases from the pyrolysis process. When the carbonization had been completed, the samples were cooled inside the oven in a N_2 atmosphere.

2.2 Carbon aerogels characterization

2.2.1 Physical gas adsorption

The textural properties were determined by obtaining and studying N_2 and CO_2 adsorption isotherms (at 77 and 273 K respectively). These isotherms were obtained with a Quantachrome Autosorb iQ2 equipment. The samples were degassed during 12 h at 393 K in high vacuum (10^{-7} mbar). N_2 adsorption isotherms were analyzed applying the BET equation (Brunauer et al. 1938). The Dubinin–Radushkevich (DR) model was applied to N_2 y CO_2 isotherms to obtain the micropore volume, W_0, and the characteristic adsorption energy, E_0. The pore average size, L_0, was obtained applying the Stoeckli equation (Stoeckli and Ballerini 1990):

$$L_0(\text{nm}) = 10.8/(E_0 - 11.4\,\text{kJ/mol}) \tag{1}$$

The volume of N_2 adsorption at a relative pressure of 0.95, $V_{0.95}$, is equivalent to the addition of the volume of micropores and mesopores, according to the Gurvitsch rule (Rouquerol et al. 2014). The mesopore volume, V_{mes}, was obtained from the difference between $V_{0.95}$ and W_0 (N_2).

2.2.2 Scanning electron microscopy

The superficial morphology of the synthesized aerogels was studied by scanning electron microscopy (SEM), employing a LEO high-resolution microscope (Carl Zeiss) GEMINI-1530 model, covering the samples with graphite and gold to enhance its conductivity and, therefore, the image resolution.

2.2.3 X-ray diffraction

It was obtained in a Panalytical PRO X'pert equipment, Cu$K\alpha$ radiation ($\lambda = 1.54060$ Å). A 10°/min sweep speed and a 0.02° step size were employed. From the diffractograms obtained, the length along the C axis (L_c) and the interplanar distance (d_{002}) for the RmC material were calculated following the Scherrer equation.

$$t = \frac{K\lambda}{D\cos\theta}$$

where t is the average size of the crystallite; K is the shape factor, taken as 0.9 in the case of carbonaceous materials; λ

is the wavelength of the X-ray radiation used, θ is the angle of the considered Bragg reflection the equipment works at and D is the line full width at half of the maximum peak intensity.

2.2.4 X-ray photoelectron spectroscopy

An ESCA 5701 spectrometer from Physical Electronics (PHI) with a radiation source $MgK\alpha$ ($hv = 1253.6$ eV) operating at 12 kV and 10 mA was employed. The samples were grinded until reaching a particle size of 100 μm and they were treated in a H_2 atmosphere at 673 K during 12 h. Then they were immersed in octane, out of contact with air, and they were transferred directly to the XPS pretreatment chamber afterwards. This way, the oxidation of Co caused by the atmospheric oxygen is avoided.

In the analysis chamber the samples were degassed at a pressure lower than 10^{-8} Torr. The spectra of the C_{1s}, O_{1s} and Co_{3p} regions were registered, and each spectral region was analyzed during the time needed to achieve a good relation signal–noise.

The analysis of the spectra obtained was carried out after the subtraction of the background by using a Shirley model (Shirley 1972). They were decomposed employing an iterative adjustment method, using Gaussian and Lorentzian functions (Voigt profile) in order to determine the number of compounds, the binding energy of the peaks (BE) and their respective areas. The binding energy of the C_{1s} peak at 284.6 eV, corresponding to C=C (aromatic–aliphatic), was taken as a reference to know the BE of the rest of the elements.

3 Results and discussion

Figure 1 shows that the aerogels prepared with catechol and phloroglucinol present type IV isotherms, characteristic of mesoporous solids. The initial part of the isotherms corresponds to the filling of the micropores present in the solid. When the relative pressure is increased, the volume adsorbed rapidly increases, due to the capillary condensation that takes place inside de mesopores (Sing et al. 1985, 2014). A H2 hysteresis loop can also be noted, corresponding to solids that have bottleneck pores, where the pore entrance is narrower than the body. The aerogel prepared with m-cresol shows an isotherm resulting from the combination of type I and IV isotherms with a H4 hysteresis loop, characteristic of solids containing slit-shaped pores.

A more detailed analysis of the textural characteristics of the materials is shown in Table 1. It is noted that only the aerogel prepared with m-cresol shows that W_0 (CO_2) > W_0 (N_2), which indicates that there are

constrictions at the narrowest micropore entrance, limiting the access of the N_2 molecule to the inside, due to the low temperature at which the adsorption takes place. Restrictions at the entrance can be due to the methyl of the m-cresol molecule, which causes blocking micropores. On the contrary, carbon aerogels prepared with catechol and phloroglucinol show W_0 (CO_2) < W_0 (N_2), and a very wide distribution in the micropore range from ultra to supermicropores; this behavior was also observed for activated carbons by Garrido et al. (1987).

The pore size distribution of porosity in the materials was determined by the density functional theory (Fig. 1). The RmC material shows a narrow distribution of smaller mesopores, whereas RC and RP show a wider distribution in large mesopores. However, the pore size distribution for the RP carbon aerogel presents two maximums in the mesopore region, which is an interesting feature for the use of this material as a molecular sieve.

It is important to point out how the porous texture of AGC changes with the type of monomer used in the synthesis of the gel. The textural differences found between materials depend on the phenolic structure that accompanies the resorcinol. The presence of the methyl group in the m-cresol produces a steric impediment in the growth of the polymer and affords lower reactivity to it, since the methyl group is not a strong activator of the aromatic ring, and therefore produces less crosslinks. On the contrary, in phloroglucinol and catechol molecules, hydroxyl groups produce less steric impediment and they are strong activators of the aromatic ring. Therefore the crosslink in the polymer is favored. As a consequence, the RmC material shows constrictions at the entrance of micropores and present lower pore volume compared to that found in RC and RP carbon aerogels (Table 1). Nevertheless, although the textural properties between RC and RP are very similar, the main difference is found in the distribution of the porosity (Fig. 1) and in the adsorption volume at $P/P_0 \sim 0.95$–1, where it is noted that RP keeps adsorbing nitrogen, which indicates the presence of large-sized mesopores.

Maldonado-Hódar et al. (2004) prepared AGC from resorcinol–formaldehyde, using cobalt acetate as a polymerization catalyst, and they found a $S_{BET} = 388$ m^2/g and V_{mes} 0.092 cm^3/g. However, when these results are compared with those of Table 1, in the case of the addition of m-cresol as a second phenol, higher micropore volume and lower mesoporosity is obtained; whereas, in the case of RC and RP materials, it is observed that the surface area is practically doubled, which confirms that the combination of these phenols produces an improvement of the textural properties of solids.

In the case of meta-cresol, which has only one hydroxyl group, methylene ether bridges are generated only in one
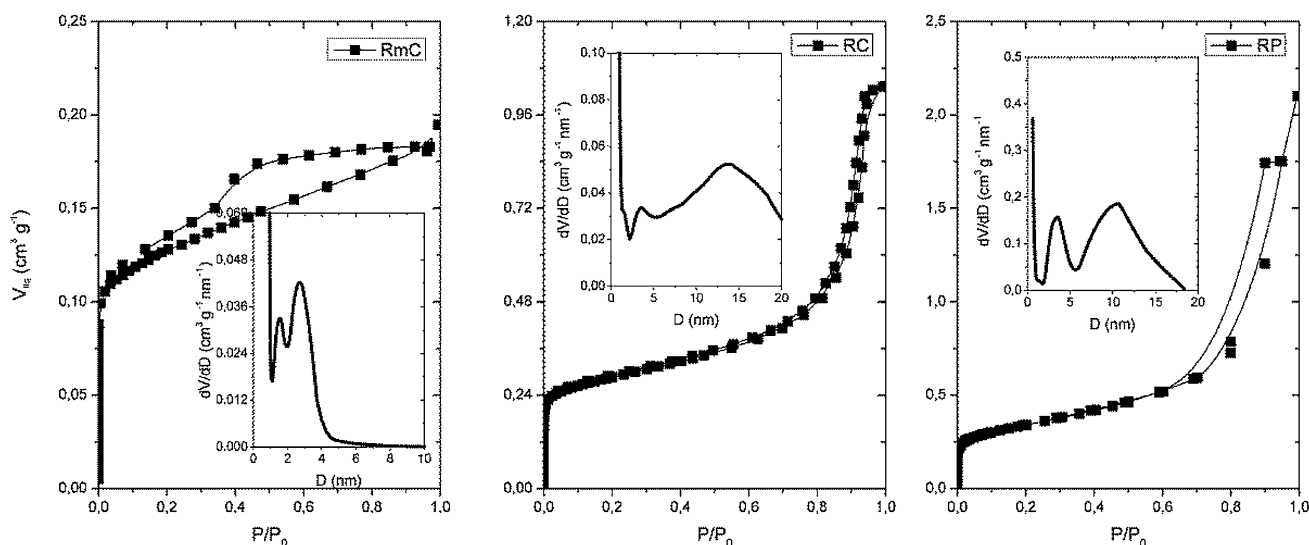
Fig. 1 N_2 adsorption isotherms at 77 K for the prepared AGC. The inserts show the distribution of the porosity obtained applying the QSDFT model to the N_2 adsorption data

Table 1 Textural characterization of AGC by N_2 and CO_2 adsorption at 77 K and 273 K respectively

Sample	N_2 at 77 K							CO_2 at 273 K	
	S_{BET} m^2/g	$V_{0.95}$ cm^3/g	SDR m^2/g	E_0 kJ/mol	V_{mes} cm^3/g	W_0 cm^3	L_0 nm	W_0 cm^3/g	L_0 nm
RmC	300	0.18	335	23.7	0.06	0.12	0.9	0.15	0.9
RC	675	0.98	742	23.3	0.76	0.26	0.9	0.24	0.6
RP	766	1.75	797	20.7	1.47	0.28	1.2	0.23	0.6

position and the degree of crosslinking is the lowest of the three gels synthesized, so that a greater collapse occurs because forces generated in the evaporation of the solvent in the course of the drying process. The lower crosslinking produce gels with lower pore volume and surface area. The collapse of the pore structure is lower due to the greater rigidity acquired in the gels prepared with catechol as monomer, in which two methylene ether bridges can be generated. In the case of using phloroglucinol, with three possible methylene ether bridges, the effect of the tensions generated during drying of the gels is even smaller and therefore gels with higher S_{BET} and $V_{0.95}$ values were obtained.

Figure 2 shows the SEM images of the AGC, where it is noted that primary particles are agglomerated due to the coalescence in the sol–gel state, which favors a more compact surface (Fairén-Jiménez et al. 2006). It is interesting noticing the formation of carbon fibers in RmC (Fig. 2a), where the phenolic methyl reduces the polymerization speed, favoring the fiber growth by stacking layers of *m*-cresol. The synthesis of carbon fibers on the surface of AGC has been studied by other authors (Fu et al. 2005; Hanzawa and Yamada 2000) employing other

conditions with the purpose of favoring the electrical properties.

Figure 3 shows the XRD of the AGC and the plans (002) and (101) of the carbonaceous material, referred to as L_c and L_a respectively. For the RmC material, it is more intense and sharp because of the graphitization of carbon fibers, which is consistent with the micrograph of Fig. 2a. For RmC, $L_c = 9.2$ nm and interplanar spacing $(d_{002}) = 0.341$ nm, which corresponds to approximately 27 aromatic layers stacked in this material (Lu et al. 2001).

Figure 4 shows XP spectra corresponding to the C_{1s} region (C=C aromatic-aliphatic, signal at 284.6 eV) and the O_{1s} region (Marchon et al. 1988). The area of the C_{1s} spectral region corresponds to superficial carbon atoms or to those with a depth between 4 and 5 nm. This spectrum presents an intense signal at 284.6 eV, followed by three signals at 285.8; 287.4 and 289.1 eV, which correspond to C–O binding energy, associated with ether groups, C=O is assigned to carbonyls, and COOR, which correspond to carboxylic groups, respectively. The fact that the C=C signal is narrower for the RmC material due to the higher graphitization degree of the sample is outstanding. Table 2 shows the percentage corresponding to each signal. It is
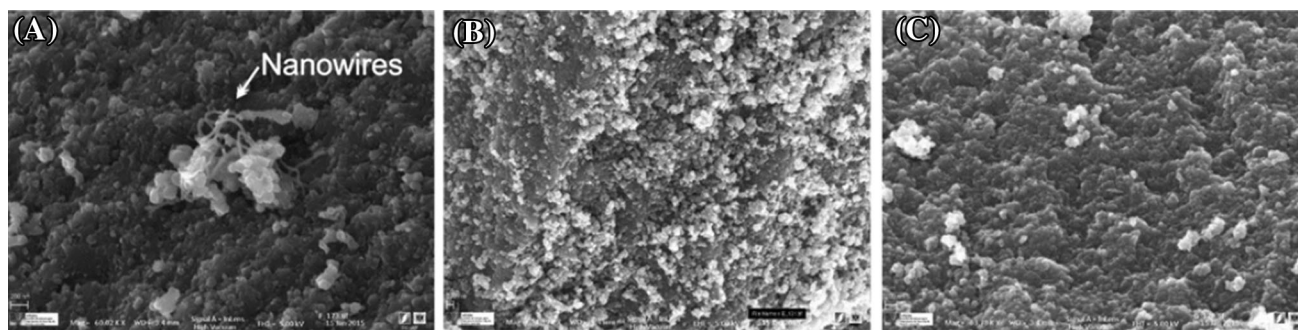
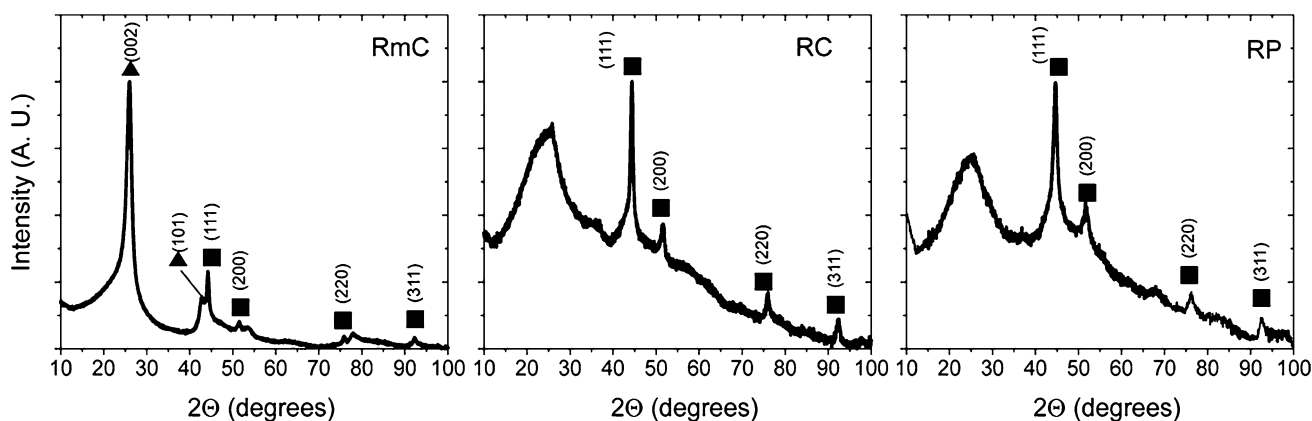Fig. 2 Micrographs of the ARGm (a RmC, b RC, c RP)

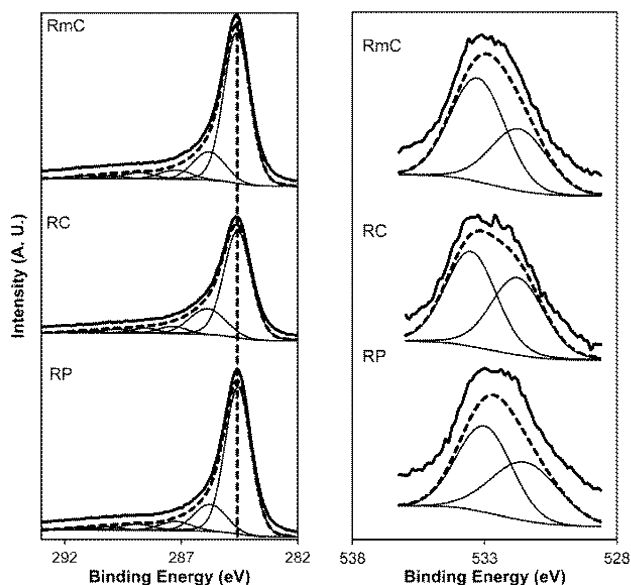Fig. 3 XRD of the AGC. Cubic Co, Carbon

Fig. 4 XP spectra of the C_{1s} region (*left*) and the O_{1s} region (*right*) of AGC

noted that, after aliphatic C=C (Aksoylu et al. 2001), ether groups are the most numerous on the surface of the solid, due to the fact that the crosslink take place through methylene and methylene-ether bridges during the polymerization process.

In the case of the O_{1s} spectral region, two signals are shown: the first one corresponds to binding energy at 531.6 eV and it is due to the presence of C=O bonds, and the second one, at 533.1 eV, is assigned to C–O bonds. According to Papirer et al. (1994), 80–90 % of the area of the O_{1s} spectral region corresponds to the contribution of superficial atoms or to atoms found in an external layer measuring from 3.5 to 4 nm.

Spectra corresponding to the Co_{2p} region are presented in Fig. 5, where the signals at 777.8–778.0 eV ($Co_{2p3/2}$) and 792.9–793.1 eV ($Co_{2p1/2}$) are observed, corresponding to Co in ground state with an approximate ΔE of 15 eV between them. It is important to point out that no other Co oxidation state is observed in the materials, as determined by means of XRD.

4 Conclusions

The porous texture of the prepared AGC and their possible applications depend on the initial mixture of phenols. The addition of *m*-cresol, as a second hydroxyl derivative,

Table 2 Percentage composition of the species determined by XPS for C$_{1s}$ and O$_{1s}$ spectral regions

Sample	Spectral region					
	C$_{1s}$ 284.6 eV	C$_{1s}$ 285.8 eV	C$_{1s}$ 287.4 eV	C$_{1s}$ 289.1 eV	O$_{1s}$ 531.4 eV	O$_{1s}$ 533.1 eV
RmC	73	16	6	2	43	57
RC	71	16	5	4	46	54
RP	73	15	5	3	44	56
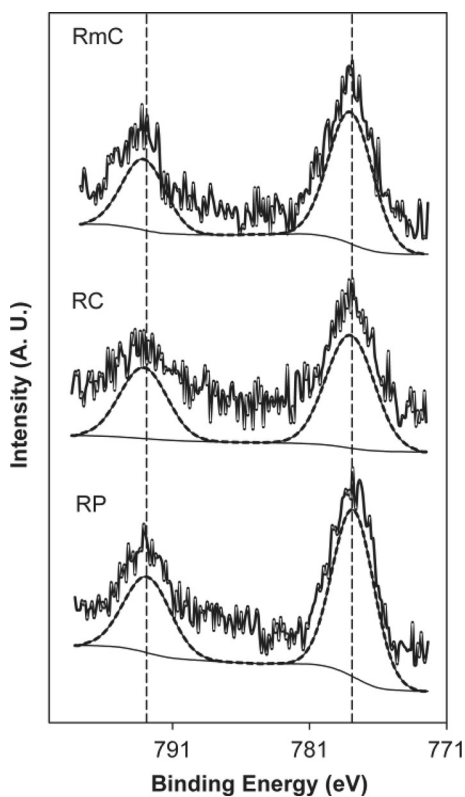
Fig. 5 XPS profile of Co$_{2p}$ region for RmC, RC and RP carbon aerogel

produces carbon aerogels with constrictions at the entrance of the micropores, due to the presence of the methyl group. RC and RP materials show the existence of a wide distribution in the micropore range, from ultra to supermicropores. The RP carbon aerogel is the only macroporous one, showing a bimodal distribution of mesopores, which makes it suitable to be used as a molecular sieve.

The use of m-cresol favors the formation of carbon fibers on the surface of AGC, which gives rise to a new kind of synthesis of these materials that enhances the properties of AGC in terms of their electrical conductivity.

References

Aksoylu, A.E., Madalena, M., Freitas, A., Pereira, M.F.R., Figueiredo, J.L.: Effects of different activated carbon supports and support modifications on the properties of Pt/AC catalysts. Carbon **39**(2), 175–185 (2001)

Brunauer, S., Emmett, P.H., Teller, E.: Adsorption of gases in multimolecular layers. J. Am. Chem. Soc. **60**(2), 309–319 (1938)

Fairén-Jiménez, D., Carrasco-Marín, F., Moreno-Castilla, C.: Porosity and surface area of monolithic carbon aerogels prepared using alkaline carbonates and organic acids as polymerization catalysts. Carbon **44**, 2301–2307 (2006)

Feng, J., Feng, J., Zhang, C.: Thermal conductivity of low density carbon aerogels. J. Porous Mater. **19**(5), 551–556 (2011)

Fu, R., Baumann, T.F., Cronin, S., Dresselhaus, G., Dresselhaus, M.S., Satcher, J.H.: Formation of graphitic structures in cobalt- and nickel-doped carbon aerogels. Langmuir **21**(7), 2647–2651 (2005)

Garrido, J., Torregrosa, R., Linares-Solano, A., Martín-Martínez, J.M., Molina-Sabio, M., Rodríguez-Reinoso, F.: Use of N$_2$ vs. CO$_2$ in the characterization of activated carbons. Langmuir **3**(1), 76–81 (1987)

Hanzawa, Y., Kaneko, K., Yoshizawa, N., Pekala, R.W., Dresselhaus, M.S.: The pore structure determination of carbon aerogels. Adsorption **4**, 187–195 (1998)

Hanzawa, Y., Yamada, Y.: Catalytic graphitization of carbon aerogels by transition metals. Langmuir **16**(9), 4367–4373 (2000)

Jirglová, H., Pérez-Cadenas, A.F., Maldonado-Hódar, F.J.: Synthesis and properties of phloroglucinol–phenol–formaldehyde carbon aerogels and xerogels. Langmuir **25**(4), 2461–2466 (2009)

Leventis, N.: Interpenetrating organic/inorganic networks of resorcinol–formaldehyde/metal oxide aerogels. In: Aegerter, M.A., Leventis, N., Matthias, M.K. (eds.) Advances in Sol–Gel Derived Materials and Technologies, vol. 1, pp. 287–313. Springer, New York (2011)

Li, W., Reichenauer, G., Fricke, J.: Carbon aerogels derived from cresol–resorcinol–formaldehyde for supercapacitors. Carbon **40**, 2955–2959 (2002)

Lu, L., Sahajwalla, V., Kong, C., Harris, D.: Quantitative X-ray diffraction analysis and its application to various coals. Carbon **39**, 1821–1833 (2001)

Maldonado-Hódar, F.J., Moreno-Castilla, C., Pérez-Cadenas, A.F.: Surface morphology, metal dispersion, and pore texture of transition metal-doped monolithic carbon aerogels and steam-activated derivatives. Microporous Mesoporous Mater. **69**, 119–125 (2004)

Maldonado-Hódar, F.J., Moreno-Castilla, C., Rivera-Utrilla, J., Ferro-Garcia, M.A.: Metal-carbon aerogels as catalysts and catalyst supports. Stud. Surf. Sci. Catal. **130**, 1007–1012 (2000)

Marchon, B., Carrazza, J., Heinemann, H., Somorjai, G.: TPD and XPS studies of O_2, CO_2, and H_2O adsorption on clean polycrystalline graphite. Carbon **26**(4), 507–514 (1988)

Moreno-Castilla, C., Maldonado-Hódar, F.J.: Carbon aerogels for catalysis applications: an overview. Carbon **43**(3), 455–465 (2005)

Papirer, E., Lacroix, R., Donnet, J.-B., Nanse, G., Fioux, P.: XPS Study of the halogenation of carbon black-part 1. Bromination. Carbon **32**(7), 1341–1358 (1994)

Pekala, R.W., Alviso, C.T.: Carbon aerogels and xerogels. Mater. Res. Symp. Process **270**, 3–14 (1992)

Pekala, R.W., Farmer, J.C., Alviso, C.T., Tran, T.D., Mayer, S.T., Miller, J.M., Dunn, B.: Carbon aerogels for electrochemical applications. J. Non-Cryst. Solids **225**, 74–80 (1998)

Rouquerol, J., Rouquerol, F., Llewellyn, P., Maurin, G., Sing, K. (eds.) Adsorption by Powders and Porous Solids: Principles, Methodology and Applications, vol. 2, p. 537. Elsevier. Oxford (2014)

Shirley, D.A.: High-resolution X-ray photoemission spectrum of the valence bands of gold. Phys. Rev. B **5**, 4709–4714 (1972)

Sing, K.S.W., Everet, D.H., Haul, R.A.W., Moscou, L., Pieroti, R.A., Rouquérol, J., Siemieniewska, T.: Reporting physisorption data for gas/solid systems with special reference to the determination of surface area and porosity. Pure Appl. Chem. **57**(4), 603–619 (1985)

Sing, K.S.W., Rouquerol, F., Rouquerol, J.: Classical interpretation of physisorption isotherms at the gas-solid interface. In: Rouquerol, J., Rouquerol, F., Llewellyn, P., Maurin, G., Sing, K. (eds.) Adsorption by Powders and Porous Solids: Principles, Methodology and Applications, vol. 2, pp. 159–189. Elsevier, Oxford (2014)

Stoeckli, F., Ballerini, L.: Evolution of microporosity during activation of carbon. Fuel **70**, 557–559 (1990)

Tamon, H., Ishizaka, H., Mikami, M., Okazaki, M.: Porous structure of organic and carbon aerogels synthesized by sol–gel polycondensation of resorcinol with formaldehyde. Carbon **35**(6), 791–796 (1997)